Sample dependence of the structural, vibrational, and electronic properties of *a*-Si:H: A density-functional-based tight-binding study

Ranber Singh

Department of Physics, Panjab University, Chandigarh, India 160014

S. Prakash

Jiwaji University, Gwalior, India 474011

Nitya Nath Shukla and R. Prasad

Department of Physics, Indian Institute of Technology, Kanpur, India 208016

In order to investigate the sample dependence of various properties of hydrogenated amorphous silicon (*a*-Si:H), we have generated four samples with 216 silicon atoms and 24 hydrogen atoms using the density functional based tight binding molecular dynamics simulations. The overall structural properties of these model samples are in agreement with the previous theoretical and experimental results. While the Si-Si and Si-H pair correlation functions are independent of preparation procedure as well as initial conditions, the H-H pair correlation functions are sample dependent. The distribution of hydrogen atoms in all the samples is nonuniform and depends upon the preparation procedure as well as the initial structure from which the hydrogenated amorphous silicon sample is generated. The Si-Si bond length and Si-Si-Si bond angle distributions are nearly independent of sample preparation procedure, but Si-H bond length distributions are sample dependent. The peaks in the vibrational density of states at high frequencies, which are due to the Si-H bond vibrations, are in reasonable accord with the experimental results. The positions of the high frequency peaks are found to be dependent on the local environment which changes from one sample to another. While the high frequency vibrational modes related to Si-Si bond vibrations are moderately localized, the vibrational modes related to Si-H bond vibrations in *a*-Si:H samples are highly localized. In samples generated from the liquid quench the free energy is smaller, whereas the entropy and specific heat are larger as compared to that of samples generated by hydrogenation of pure amorphous silicon samples. The total electronic density of states and local density of electronic states (LDOS) at Si atom sites are nearly sample independent, while the LDOS at the H atom sites are dependent on the sample preparation procedure.

I. INTRODUCTION

Hydrogenated amorphous silicon (*a*-Si:H), technologically an important material which suffers from the light-induced degradation [Staebler-Wronski effect[1]], has been studied extensively both experimentally and theoretically.[2] However, the issues related to its various microscopic properties such as coordination defects,[3] vibrational localization,[4] lifetime and decay of phonons,[5] electronic gap states,[6,7] distribution and dynamics of hydrogen[8–15] are still the subjects of debate. Several studies show that this material exhibits structural inhomogeneities.[11,16,17] The study of pure and hydrogenated amorphous silicon is also important from other perspectives as these are prototypes of disordered covalent semiconducting materials.

a-Si:H can be grown by various techniques including sputtering[18] and plasma enhanced chemical vapor deposition.[19] For experimental studies and practical applications it is grown in thin films,[20] whereas for theoretical studies it is generated by using systematic computer simulation techniques. These techniques make use of empirical[21–23] or *ab intio* pseudo potentials[24] in conjunction with Monte Carlo[25,26] and MD simulations[27–30] which allow simulations of thermal treatments similar to those used in laboratories to prepare the actual samples. Currently, there are many realistic atomic models of pure amorphous silicon available (up to 100,000 atoms[31]) which have been generated by using the continuous random network forming computer algorithms.[25,26] However, due to difficulties in modeling the interactions of hydrogen in the bulk silicon and a small time step needed for the dynamics of hydrogen, the modeling of hydrogenated amorphous silicon is limited and has been achieved mainly by MD simulations.[32–36] Moreover, the theoretical understanding of its various structural, vibrational and electronic properties is still not complete and provides motivation for extensive studies.

Due to its non-equilibrated nature, *a*-Si:H shows a variation in its properties depending on the sample preparation conditions. In this paper we address the question of dependence of various properties of *a*-Si:H on the preparation conditions. We have generated four samples of *a*-Si:H with 216 Si atoms and 24 H atoms using the density functional based tight binding (DFTB) approach.[37] Two samples of *a*-Si:H are generated from the liquid quench at two different quenching rates while the other two are generated by the hydrogenation of two different pure amorphous silicon samples. One sample of pure amorphous silicon is generated from the liquid quench by the same DFTB approach while

the other one is due to Wooten *et al.*.[25] Frauenheim *et al.* have successfully used the DFTB approach[37] to generate the structure of *a*-Si:H (120 Si and 8 H atoms) and studied its structural and dynamical properties.[38] But in this paper, we studied the sample dependence of the structural, vibrational and electronic properties of various samples of *a*-Si:H generated by using the same DFTB approach.

The paper is organized as follows. The computational details of methods used for generating samples and subsequent calculations of dynamical matrix, localization of vibrational modes, vibrational density of states (VDOS), thermodynamic properties from the VDOS and electronic density of states are given in Sec. II. The results of our calculations are discussed in Sec. III and summarized in Sec. IV.

II. COMPUTATIONAL DETAILS

For the structural relaxation, we sample the Brillouin zone of the supercell lattice at the Γ point alone and adopt the canonical ensemble scheme where the kinetic energy of the ionic motions is constantly rescaled to the simulation temperature. In the stimulated annealing mode of the MD program, the force tolerance threshold is set to 0.0001 (atomic units) and the electronic temperature for Fermi broadening to 300 K. We used *sp*-basis set for Si and *s*-basis set for H. The range of repulsive potential and cut-off distance for the next nearest neighbor (in atomic units) respectively are 4.8 and 4.8 for Si-Si interactions, 3.2 and 3.2 for Si-H interactions, 2.99 and 2.0 for H-H interactions. The ionic motions are calculated with discrete time steps of about 1 fs. For the generation of structures of pure and hydrogenated amorphous silicon from liquid quench, we used the dynamical method. In this method we start with crystalline sample then raise the temperature of the sample to 4000 K. The sample is then equilibrated at 4000 K for 0.5 ps to destroy the memories of its initial structure and then cooled down to 1800 K in 2 ps to form a liquid where it is equilibrated for further 2 ps. The cell is then quenched to 300 K where it is equilibrated for some more time. The samples of pure and hydrogenated amorphous silicon with 216 silicon atoms and 24 hydrogen atoms are generated within a simple cubic simulation cell of side 16.2813 Å. We have taken the simulation cell of size 16.2813 Å to have the same mass density of pure amorphous silicon sample as that of WWW model sample.[25] The hydrogen atoms are added into the initial crystalline silicon by dividing the simulation cell into 27 equal cubes and placing hydrogen atoms at tetrahedral positions, one in each of 24 of the 26 outer cubes. While two samples of *a*-Si:H are generated from the liquid quench at two different quenching rates, two more samples are generated by the hydrogenation of pure amorphous silicon samples. These samples are labeled as follows.

ASi: Pure amorphous silicon sample generated by using a quenching rate of 2×10^{14} K/s from the liquid state at 1800 to 300 K where it is further equilibrated for 2.5 ps.

ASiH: *a*-Si:H sample generated by using a quenching rate of 2×10^{14} K/s from the liquid state at 1800 to 300 K where it is further equilibrated for 2.5 ps. At 300 K the diffusion almost ceases. Therefore, to relax the structure further

the temperature is raised to 1200 K, equilibrated there for 1 ps and then cooled again to 300 K at the rate of 4 $\times 10^{14}$ K/s. At 300 K, it is equilibrated for 2.0 ps.

BSiH: *a*-Si:H sample generated by using a quenching rate of 4×10^{14} K/s from the liquid state at 1800 to 1200 K where it is equilibrated for 1 ps and then cooled down to 300 K at the same rate. At 300 K it is further equilibrated for 5 ps. The structure is further relaxed by raising the temperature to 1200 K where it is equilibrated for 1 ps and then cooled to 300 K at the rate of 4×10^{14} K/s. At 300 K, it is again equilibrated for 2.0 ps.

CSiH: *a*-Si:H sample generated by hydrogenation of *ASi* sample of pure amorphous silicon. This is done by dividing the simulation cell into 27 equal cubes and placing hydrogen atoms at arbitrary positions in 24 of the 26 outer cubes. The resultant structure is simulated for 0.5 ps at 300 K. To increase the diffusion of atoms, the temperature is raised to 1200 K at the rate of 6×10^{14} K/s where it is equilibrated again for 1 ps and then cooled to 300 K at the rate of 2 $\times 10^{14}$ K/s. At 300 K, it is again equilibrated for 2.5 ps.

WSiH: *a*-Si:H sample generated by hydrogenation of WWW sample of pure amorphous silicon of Wooten *et al.*[25] adopting the same procedure as for CSiH.

To investigate the vibrational properties of the above samples, the dynamical matrix is constructed with the help of the differentiation scheme defined as

$$D_{jl}^{xy} = \frac{\delta^2 E_{jl}}{\delta x \delta y} = \frac{\delta F_{jl}^y}{\delta x} = \frac{F_{jl}^{y^+} - F_{jl}^{y^-}}{2\Delta}, \qquad (1)$$

where, $F_{jl}^{y^+}$ ($F_{jl}^{y^-}$) refers to the *y*-component of the interaction force between the atoms *j* and *l* when the distance between them is increased (decreased) in any arbitrary Cartesian direction (*x*) by a sufficiently small displacement Δ. In our calculations we have taken $\Delta = 0.005$ Å. The diagonalization of this dynamical matrix gives the eigenvalues (square of vibrational frequencies) and the eigenvectors (vibrational patterns) which are further used to calculate the VDOS and localization of vibrational modes of the model samples. The broadening width of 20 cm^{-1} is used to calculate the VDOS. Once the information of VDOS is available, it is easy to construct the temperature dependence of thermodynamic properties. In the harmonic approximation the free energy (*F*), entropy (*S*) and specific heat (*C*) per atom of a simulated system are calculated using the following expressions:[39]

$$F = 3k_BT \int_0^\infty \ln\left\{ 2\sinh\left(\frac{\hbar\omega}{2k_BT}\right) \right\} g(\omega) d\omega, \qquad (2)$$

$$S = 3k_B \int_0^\infty \left[\frac{\hbar\omega}{2k_BT} \coth\frac{\hbar\omega}{2k_BT} - \ln\left(2\sinh\frac{\hbar\omega}{2k_BT} \right) \right] g(\omega) d\omega,$$

$$(3)$$

$$C = 3k_B \int_0^\infty \left(\frac{\hbar\omega}{k_B T}\right)^2 \left(\frac{e^{\hbar\omega/k_B T}}{(e^{\hbar\omega/k_B T}-1)^2}\right) g(\omega)d\omega, \qquad (4)$$

where $g(\omega)$ is VDOS normalized to unity. k_B is the Boltzmann constant, T is the temperature, $\hbar$ is the Planck's constant and the other symbols have their usual meanings. However, the vibrational excitations with wavelengths longer than the size of the supercell cannot be excited in the model sample and will be missing in its VDOS data. Thus, such calculations of thermodynamic properties will not incorporate the effects of low frequency modes as well as the modes which are anharmonic in nature.

The localization behavior of the vibrational modes is investigated by calculating the inverse participation ratio (IPR) which for a vibrational mode j is defined as[40]

$$\text{IPR} \equiv P_j = \left[\frac{(\sum_i |u_i^j|^2)^2}{\sum_i |u_i^j|^4}\right]^{-1}, \qquad (5)$$

where u_i^j is the displacement of ith atom from its equilibrium position in the jth vibrational mode and the sum is over all the N atoms in the model sample. The IPR varies from $1/N$ (all atoms have equal vibrational amplitude) to 1 (only a single atom has considerable vibrational amplitude). If all the atoms have nearly equal vibrational amplitudes in a particular vibrational mode, the mode is called an extended mode and if only a few atoms have a considerable vibrational amplitude, then the mode is said to be localized. Thus, a vibrational mode for which the IPR is approaching 1 will be a localized mode.

For the electronic structure calculations of the above model structures, a huge memory is required. Therefore, we could use the maximum of 16 k-points of the Brillouin zone. For the calculation of electronic density of states we have used $2 \times 2 \times 2$ Monkhorst-Pack[41] mesh of k-points.

III. RESULTS AND DISCUSSION

A. Structural properties

We first discuss the structural properties of the four a-Si:H samples with the help of Figs. 1–5 and Tables I–III. The data, as given in these figures and tables, are the averages of 100 configurations over a time span of 0.5 ps. The pair correlation function for the pure amorphous silicon as given in Fig. 1 shows a good agreement with the experimental data.[42] The first peak which corresponds to the first nearest neighbours is sharp and occurs at 2.37 Å. However, the second and third peaks corresponding to the second and third nearest neighbors are broader. The partial pair correlation functions of Si-Si, Si-H and H-H correlations in a-Si:H samples (ASiH, BSiH, CSiH and WSiH) are given in Fig. 2. In Si-Si and Si-H pair correlation functions, the first peaks corresponding to Si-Si and Si-H bond lengths are sharp. However, in H-H pair correlation function it is broadened and occurs above 2.0 Å, which indicates the nonexistence of molecular hydrogen (bond length ≈ 1.0 Å) but the hydrogen configurations with two hydrogen atoms spaced more than
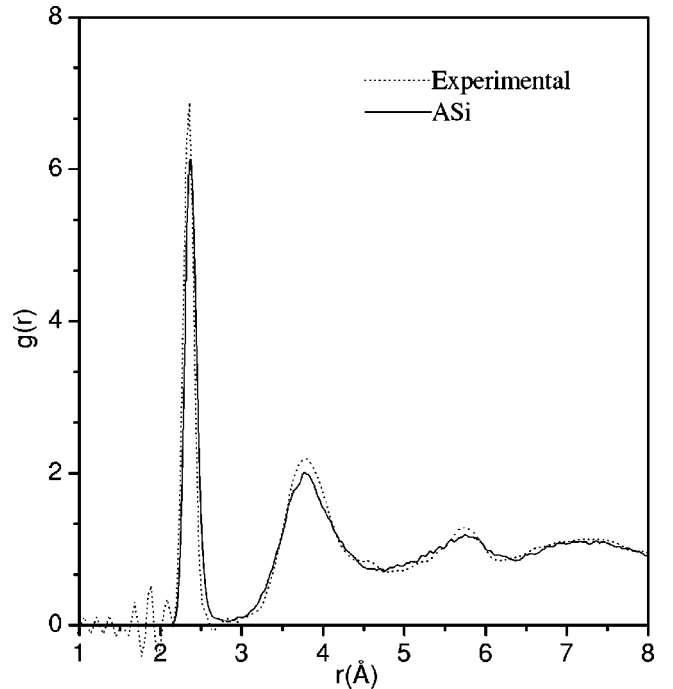

FIG. 1. The Si-Si pair correlation function, $g(r)$, of pure amorphous silicon sample (ASi) along with the experimental data (Ref. 42).

2.0 Å apart and/ or clustering of hydrogen atoms in a-Si:H. This is in agreement with the *ab initio* results[32] as well as the experimental data.[43] The second and third nearest neighbor peaks in Si-Si and Si-H correlation functions in the a-Si:H sample are broader. In H-H correlation functions there is no clear peak except the first peak. The positions of main peaks in the pair correlation functions of different samples are given in Table I, where the data from the previous theoretical[25,32,44] and experimental[42,43] studies are also given for comparison. There is a good agreement between the positions of peaks in the pair correlation functions of our samples and the experimental data.

From Fig. 2, it is also clear that as far as Si-Si and Si-H pair correlation functions are concerned all the four samples (ASiH, BSiH, CSiH and WSiH) are quite similar. This shows that Si-Si and Si-H pair correlation functions are independent of the preparation procedure and initial structure from which the hydrogenated sample is generated. However, the H-H pair correlation functions show the dependence on preparation procedure. The overall behavior of H-H pair correlation functions is quite similar to the experimental results.[43] However, due to the finite size of the samples and a small number of hydrogen atoms, the statistics is not good enough to draw any general conclusion except that the distribution of hydrogen in amorphous silicon is nonuniform and depends upon the preparation procedure and initial structure from which the hydrogenated sample is generated. A small angle neutron scattering study[11] of nonuniform hydrogen distribution in a-Si:H has also reported the existence of hydrogen heterogeneity on nanometer scale in a-Si:H.

A more detailed structural description of the model samples is given by the bond length and bond angle distri-
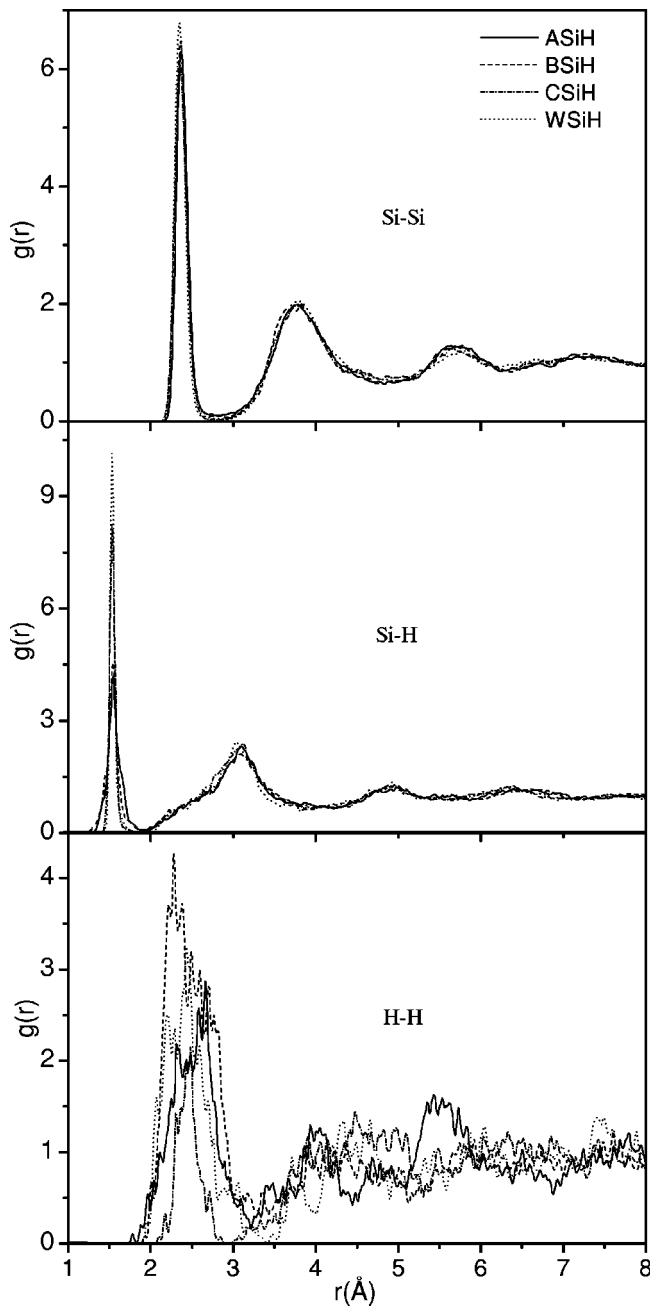
FIG. 2. The partial pair correlation functions, $g(r)$, of Si-Si, Si-H and H-H correlations in a-Si:H samples (ASiH, BSiH, CSiH and WSiH). The labeling of all the curves in the middle and bottom panels is the same as in the top panel.

FIG. 3. The distribution functions of (a) Si-Si bond length and (b) Si-Si-Si bond angle in ASi and WWW samples.

butions. These distributions for pure and hydrogenated amorphous silicon samples are calculated by defining the cut-off distances for Si-Si and Si-H bondings up to the first minima in their respective correlation functions. The Si-Si bond length and Si-Si-Si bond angle distributions for ASi and WWW samples are shown in Fig 3. These distribution functions show a broad distribution with peaks, respectively, at around 2.37 Å and 106°. The distribution functions for ASi and WWW samples are in good agreement except some noise in the curves corresponding to WWW sample. This is because of the fact that for WWW sample only one configu-
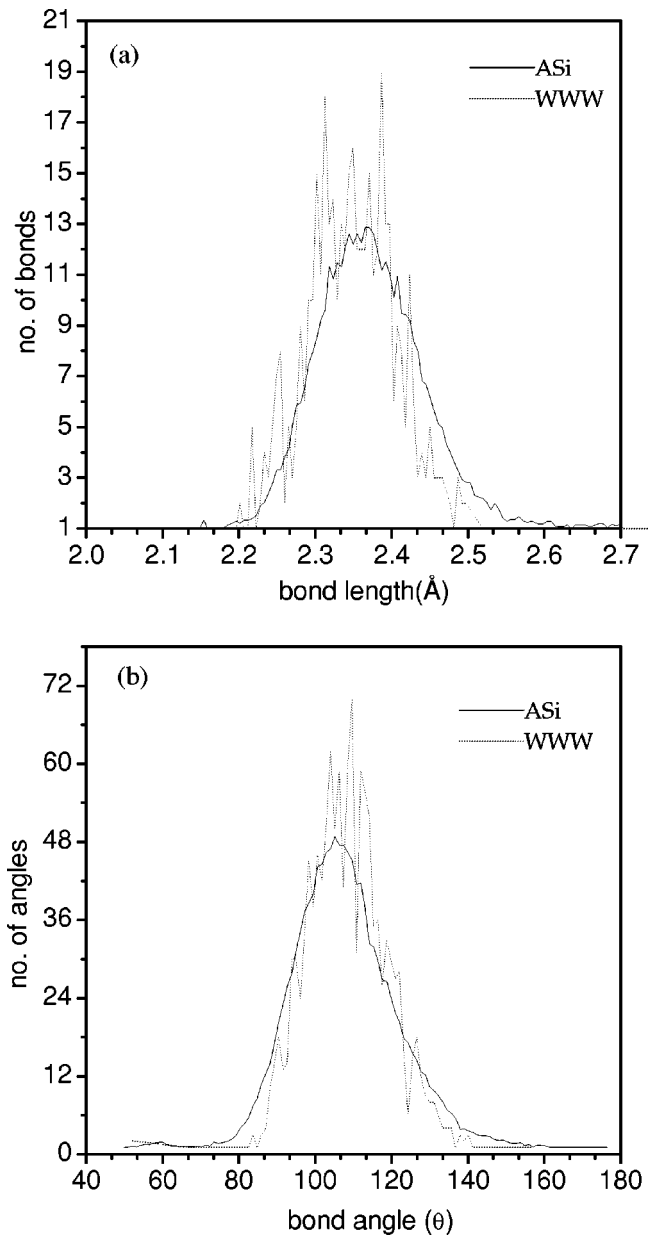
ration was used while for ASi sample the average was taken over 100 configurations. These distributions indicate that ASi sample deviates from the perfect tetrahedral network and has a distribution over bond length and bond angle. The root mean square deviations (RMD) of Si-Si bond length and Si-Si-Si bond angle distributions in ASi and WWW samples are 0.13 Å and 16.65°, and 0.08 Å and 11.19°, respectively.

Figure 4 shows that the Si-Si bond length and Si-Si-Si bond angle distribution functions in WSiH sample have sharper peaks as compared to other samples. These peaks occur respectively at about 2.34 Å and 108°, which are quite close to the corresponding values in crystalline silicon. It indicates that the WSiH sample has crystalline features which is due to the already present crystalline components in the model structure of WWW sample as has been shown by Wooten *et al.*[25] These distribution functions in ASiH, BSiH
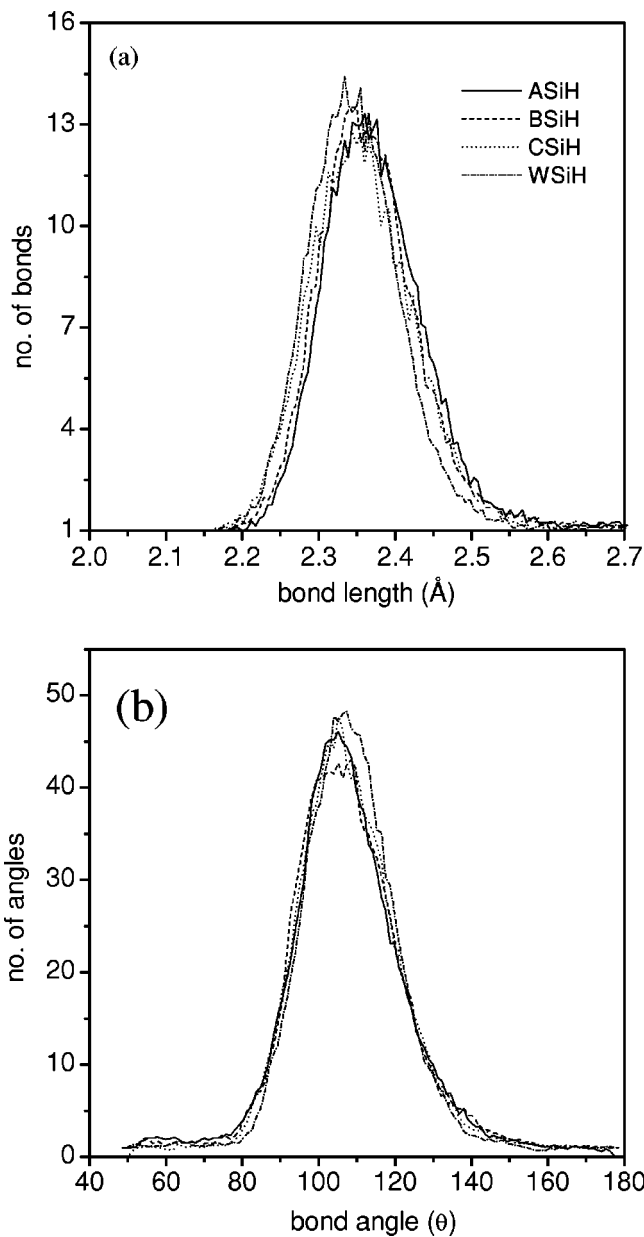
FIG. 4. The distribution functions of (a) Si-Si bond length and (b) Si-Si-Si bond angle in a-Si:H samples (ASiH, BSiH, CSiH and WSiH). The labeling of all the curves in the bottom panel is the same as in the top panel.
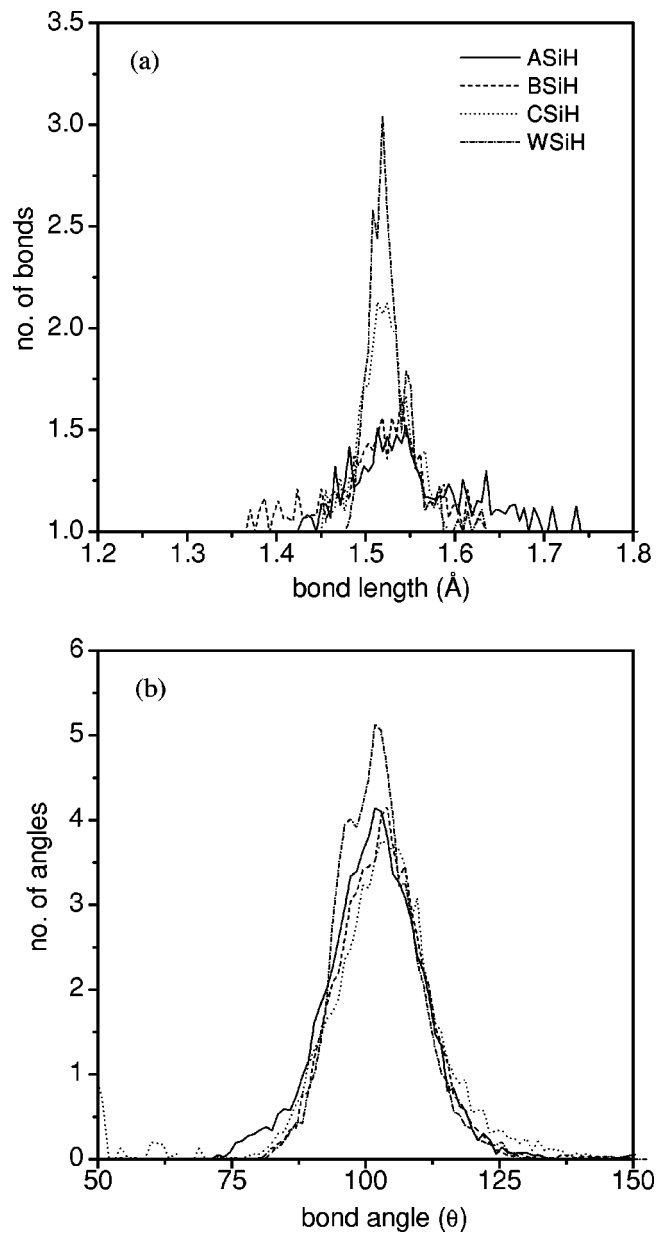

FIG. 5. The distribution functions of (a) Si-H bond length, and (b) Si-Si-H bond angle in a-Si:H samples (ASiH, BSiH, CSiH and WSiH). The labeling of all the curves in the bottom panel is the same as in the top panel.

and CSiH samples are nearly identical with a little variation in their peak heights and positions occurring at around 2.36 Å and 106°, respectively. Thus, Si-Si bond length and Si-Si-Si bond angle distributions are almost independent of preparation procedure and the initial structure from which the hydrogenated sample is generated. The RMD of Si-Si bond length and Si-Si-Si bond angle distributions in ASiH, BSiH, CSiH and WSiH samples are 0.12 Å and 17.15°, 0.11 Å and 17.37°, 0.13 Å and 15.79°, and 0.11 Å and 15.61°, respectively.

The Si-H bond length distributions (see Fig. 5) are different in all the samples except that the peak occurs nearly at about 1.52 Å. In a-Si:H samples generated from the liquid quench, this distribution is broader whereas it is sharper in

the samples prepared by hydrogenation of pure amorphous silicon. This can be attributed to the stability of Si-H bonding in these samples. As these distribution functions are the time averages, the broader distribution indicates that Si-H bonding is unstable so that bond length has a variation over a certain range, while the narrow distribution indicates that the Si-H bonding is relatively stable and there is little variation in the bond length. The comparison of the Si-H bonding distributions for ASiH and BSiH samples also shows that the distribution is sharper for BSiH sample prepared by the faster quenching rate. The Si-Si-H bond angle distributions (see Fig. 5) are nearly similar in all samples except that it is sharper in WSiH sample. The sharper peak is due to the presence of crystalline components in the structure of WSiH

TABLE I. The positions of peaks in Si-Si, Si-H and H-H pair correlation functions of our samples as shown in Figs. 1 and 2. All the values are in Å. The data available from the previous theoretical (Ref. 25, 32, and 44) and experimental (Refs. 42 and 43) studies are also given for comparison.

Samples/peaks	Si-Si			Si-H			H-H
	I	II	III	I	II	III	I
Amorphous silicon[42]	2.36	3.77	5.74				
WWW[25]	2.36	3.82	5.80				
ASi	2.37	3.77	5.75				
a-Si:H[43]	2.37	3.78	5.64	1.48	3.13	4.85	2.38-2.70
a-Si:H[32]	2.35	3.80	-	1.59	3.12	-	2.20-2.60
a-Si:H[44]	2.37	3.72	-	1.59	3.18	5.25	2.00-4.00
ASiH	2.37	3.78	5.71	1.54	3.10	4.91	2.31-2.66
BSiH	2.36	3.83	5.77	1.54	3.09	4.97	2.21-2.38
CSiH	2.36	3.81	5.65	1.53	3.12	4.91	2.30-2.48
WSiH	2.35	3.80	5.79	1.53	3.04	4.91	2.20-2.43

sample as shown above by the Si-Si bond length and Si-Si-Si bond angle distribution functions given in Fig. 4. Thus, Fig. 5 indicates that while the Si-H bond length distributions are dependent upon the preparation procedure as well as the initial structure from which the hydrogenated sample is generated, the Si-Si-H bond angle distributions are nearly independent.

In addition to the four-fold Si atoms there are also three-fold and five-fold Si atoms in our samples as given in Table II. In ASi sample the average percentages of three-fold, four-fold and five-fold Si atoms are, respectively, 3.08, 90.85, and 5.91, while in WWW model these are 0.00, 99.10 and 0.90. Upon hydrogenation, these values become nearly similar in both samples, i.e., 2.41, 95.52 and 2.07 in CSiH sample and 1.84, 95.85 and 2.29 in WSiH sample. The *a*-Si:H samples (ASiH, BSiH) generated from the liquid quench have more coordination defects (three fold and five fold atoms) than those (CSiH, WSiH) generated by hydrogenation of pure amorphous silicon samples. Thus the samples generated from the liquid quench are found to be more disordered as compared to those generated by hydrogenation of pure amorphous silicon samples. The comparison of coordination defects in ASiH and BSiH samples shows that the sample

(BSiH) prepared by the faster quenching rate has less coordination defects than that prepared at the slower rate.

The mean coordination numbers, Z_{Si-Si}, Z_{Si-H}, Z_{H-Si} and $Z_{tot}(=Z_{Si-Si}+Z_{Si-H})$ are given in Table II. The data available from the previous theoretical studies[25,32] are also given for comparison. The total coordination number, Z_{tot}, of a Si atom in all the samples is nearly equal to 4. The Z_{Si-Si} of a Si atom in ASi sample is 4.03, which is quite close to 4.01 of WWW model.[25] However, upon hydrogenation it reduces to 3.89 in both the samples (CSiH and WSiH). The Z_{Si-Si} and Z_{tot} of a Si atom in ASiH and BSiH samples is larger than that of CSiH and WSiH samples. This indicates that a Si atom in ASiH and BSiH samples is more over-coordinated as compared to that in CSiH and WSiH samples. The Z_{H-Si} of a hydrogen atom in all the *a*-Si:H samples is nearly equal to 1.0, which means that almost all the hydrogen atoms are bonded to silicon atoms as Si-H monohydrides. This is in agreement with the vibrational spectroscopy results.[45,46] Further, we found that Si-H monohydrides exist either as isolated Si-H configurations or as the clusters of Si-H monohydrides. The Si-H clustering has also been observed in experiment[47] and computer simulations.[10,32,36,48]

TABLE II. The average percentages of *n*-fold (3, 4, 5) Si atoms and the mean coordination numbers Z_{Si-Si}, Z_{Si-H}, Z_{H-Si} and $Z_{tot}(=Z_{Si-Si}+Z_{Si-H})$ in our samples. The average is taken of 100 configurations over a time span of 0.5 ps. The available data from the previous theoretical (Refs. 25 and 32 studies are also given for comparison.

Samples	3	4	5	Z_{Si-Si}	Z_{Si-H}	Z_{H-Si}	Z_{tot}
WWW[25]	0.00	99.10	0.90	4.01	-	-	4.01
ASi	3.08	90.85	5.91	4.03	-	-	4.03
a-Si:H[32]	1.00	91.50	7.50	3.90	0.13	1.00	4.03
ASiH	4.47	88.20	7.33	3.92	0.12	1.04	4.04
BSiH	3.58	90.81	5.61	3.91	0.11	1.00	4.02
CSiH	2.41	95.52	2.07	3.89	0.11	1.00	4.00
WSiH	1.84	95.85	2.29	3.89	0.12	1.04	4.01

The average values of mean bond lengths (Si-Si and Si-H) and mean bond angles (Si-Si-Si, Si-Si-H, Si-H-Si and H-Si-H) are given in Table III. The Si-Si bond length in ASi sample is 2.38 Å compared to 2.35 Å in WWW model and 2.35 Å in crystalline silicon. In the a-Si:H samples viz. ASiH, BSiH, CSiH and WSiH, it is, respectively, 2.39, 2.38, 2.36 and 2.36 Å. This shows that in ASiH and BSiH samples, the Si-Si bond length is nearly equal to that in the ASi sample, but in other hydrogenated samples it is smaller. This decrease in Si-Si bond length can be attributed to the relaxation of strain associated with the weak Si-Si bonds upon hydrogenation. The Si-H bond length in ASiH, BSiH, CSiH and WSiH samples is 1.56, 1.54, 1.53 and 1.53 Å, respectively. The comparison of Si-Si and Si-H bond lengths in a-Si:H samples indicates that these bond lengths are larger in the samples (ASiH, BSiH) prepared from the liquid quench compared to the samples (CSiH, WSiH) prepared by hydrogenation of pure amorphous silicon samples. This means that the samples prepared by hydrogenation of pure amorphous silicon have less strain compared to the samples prepared from liquid quench. However, the comparison of Si-Si and Si-H bond lengths in ASiH and BSiH samples indicates that BSiH sample has less strain compared to ASiH sample. The mean Si-Si-Si bond angle in ASi sample is 108.23° compared to 109.12° in WWW model and 109.47° in crystalline silicon. In ASiH and BSiH samples it is nearly equal to 108°, while in CSiH and WSiH samples it is 108.8°. This indicates that CSiH and WSiH samples are closer to the perfect tetrahedral network. The mean Si-Si-H bond angle is less than Si-Si-Si bond angle, i.e., 103.20, 103.81, 104.67 and 102.79°, respectively, in ASiH, BSiH, CSiH and WSiH samples. This means that three Si atoms bonded to a hydrogen bonded Si atom have the tendency to have a planar structure. There exists stable Si-H-Si bridge configuration in ASiH and WSiH samples with Si-H-Si bond angle nearly equal to 157°. Such stable Si-H-Si bridge configuration does not exist in BSiH and CSiH samples. However in CSiH sample, it forms, stays for some time and then breaks with the average Si-H-Si angle of 114.36° over a time span of 0.5 ps. In ASiH and BSiH samples, there also exist SiH$_2$ configurations with average H-Si-H bond angle equal to 107.90° and 102.25°, respectively.
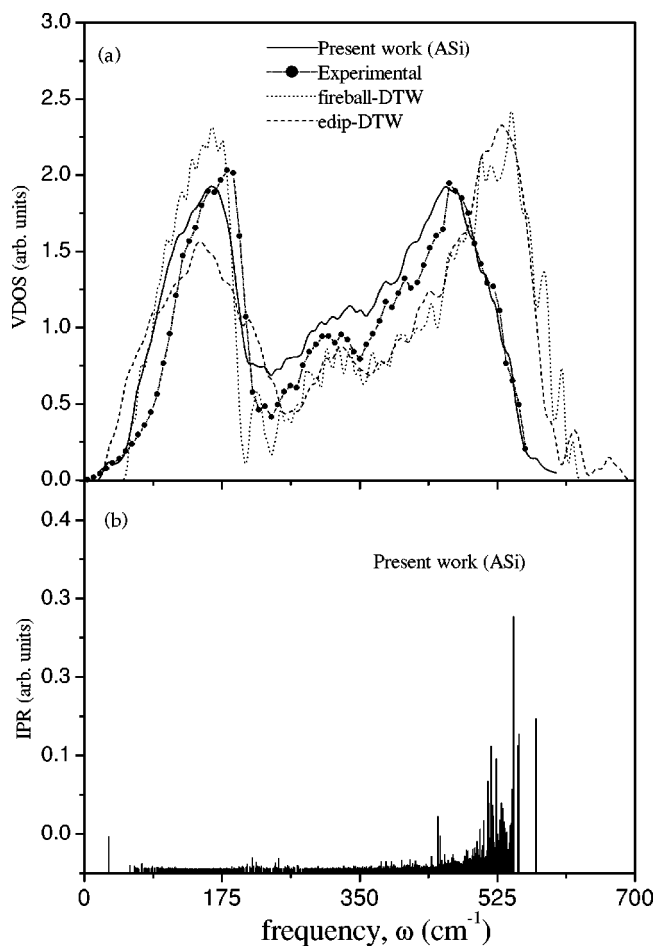

FIG. 6. (a) The comparison of vibrational density of states (VDOS) of our sample (ASi) of pure amorphous silicon with the experimental (Ref. 49) and other model samples (fireball-DTW—Ref. 50, edip-DTW—Ref. 51). (b) The inverse participation ratio (IPR) of ASi sample indicating that the high frequency modes are localized.

B. Vibrational properties

The VDOS of ASi sample of pure amorphous silicon is given in Fig. 6(a). Also shown in Fig. 6(a) are experimental[49] and theoretical[50,51] results. Our calculations are in good

TABLE III. The average mean bond lengths (Si-Si and Si-H) in Å and mean bond angles in degrees (Si-Si-Si, Si-Si-H, Si-H-Si and H-Si-H). The average is taken of 100 configurations over a time span of 0.5 ps. The bridge Si-H-Si configuration does not exist in BSiH sample while H-Si-H configuration exist only in ASiH and BSiH samples. The root mean square deviations in the Si-Si bond length (Δr) and Si-Si-Si bond angle distributions ($\Delta\theta$) are also given.

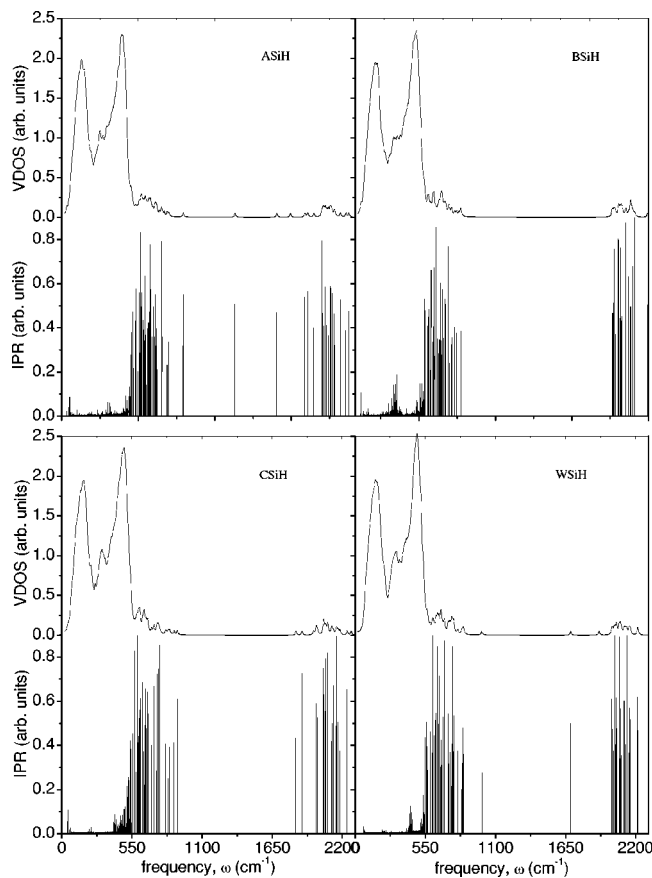| Samples	Si-Si	Δr	Si-H	Si-Si-Si	$\Delta\theta$	Si-Si-H	Si-H-Si	H-Si-H
WWW	2.35	0.08		108.57	11.19			
ASi	2.38	0.13		108.23	16.65			
ASiH	2.39	0.12	1.556	107.93	17.15	103.20	157.15	107.90
BSiH	2.38	0.11	1.535	108.17	17.37	103.81	-	102.25
CSiH	2.36	0.13	1.531	108.79	15.79	104.67	114.36	-
WSiH	2.36	0.11	1.532	108.80	15.61	102.79	156.75	-

FIG. 7. The VDOS and IPR of vibrational modes in *a*-Si:H samples (ASiH, BSiH, CSiH and WSiH). For clarity these are displayed separately for each sample.

agreement with the experimental data in the whole frequency range. We note that previous theoretical results[50,51] do not compare well with the experimental results. In the fireball-DTW[50] results, the low frequency peak is larger while in edip-DTW[51] results it is smaller than that of the experimental data. However, the high frequency peak in VDOS of both fireball-DTW and edip-DTW results is at higher frequencies compared to the experimental data. The IPR of vibrational modes [see Fig. 6(b)] shows that the high frequency modes are localized in ASi sample. Similar conclusions have also been reported by other authors.[40,50,52] Due to the finite size of our ASi sample, the vibrational modes below 50 cm^{-1} are missing but we have found one localized mode at around 30 cm^{-1}. Such localized mode could arise due to the presence of voids in the sample as has been reported by Nakhmanson *et al.*[50] in amorphous silicon.

The calculated VDOS and IPR of vibrational modes in the hydrogenated samples (ASiH, BSiH, CSiH and WSiH) are shown in Fig. 7. For clarity, we have displayed them separately for each sample. The main peaks in VDOS of all the hydrogenated samples lie below 550 cm^{-1} and are almost similar. The small peaks due to the Si-H vibrational modes above the main peaks lie in the frequency range of 600–900 cm^{-1} and 1900–2200 cm^{-1} in all samples and their locations change from sample to sample. There are three types of Si-H vibrational modes in amorphous silicon: (i)

wagging modes (630–650 cm^{-1}), (ii) bending modes (830–860 cm^{-1}), and (iii) stretching modes (2000–2200 cm^{-1}). The dominating peaks are at around 626, 840, 2053 and 2107 cm^{-1} in ASiH; 661, 830, 2035, 2085 cm^{-1} in BSiH; 645, 2054, 2117 cm^{-1} in CSiH and 646, 2049, 2114 cm^{-1} in WSiH. This indicates that the Si–H vibrations are sensitive to the local environment as it changes from one sample to another. The experimental measurement of VDOS of *a*-Si:H[53] has shown the existence of extra peaks in VDOS at about 646, 889, 2000, 2100 cm^{-1}, respectively, which have been attributed to the wagging modes of hydrogen, bending modes of SiH$_2$ configuration, stretching mode of SiH and stretching mode of SiH$_2$ vibrations. The Raman spectra of *a*-Si:H[54] shows these peaks at 640, 2000, 2100 cm^{-1}. Mauseau *et al.*[55] also calculated the VDOS of hydrogen atoms in *a*-Si:H and identified three main peaks at 645, 888, 2100 cm^{-1}. In the IR spectra of *a*-Si:H,[12,45,56] the (Si-H)$_x$ hydride vibrations have characteristic absorptions at 630–650 cm^{-1} (wagging mode), 840–890 cm^{-1} (bending scissor mode of H-Si-H), 1980–2030 cm^{-1} (Si-H stretching mode), 2060–2160 cm^{-1} (H-Si-H stretching mode and/or clusters of Si-H monohydrides).

The IPR of vibrational modes in different hydrogenated samples in Fig. 7 shows that the localization of vibrational modes below 575 cm^{-1} in all the hydrogenated samples is almost similar to that in the pure amorphous silicon sample [Fig. 6(b)]. However, the vibrational modes above 575 cm^{-1} which are mainly related to Si-H bond vibrations are highly localized. Recently, Rella *et al.*[4] have also reported that Si-H stretch vibrations are highly localized. The comparison of IPR of Si-H vibrational modes in different samples also indicates that their localization is sensitive to the local environment as it changes from one sample to another. Similar to ASi sample, in *a*-Si:H samples also there are some localized modes below 50 cm^{-1} which may be arising due to the presence of voids in the samples.

In the amorphous solids there exist some universal features, for example, a bump in the low-temperature specific heat[57] and an excess of low frequency modes (about 20–120 cm^{-1}) in the Raman and neutron scattering spectra.[58] In the neutron scattering spectra, it is usually expressed as a peak in VDOS/ω^2. We displayed VDOS/ω^2 plots for our samples of pure and hydrogenated amorphous silicon in Fig. 8. We find that there occurs a broad band peak with two small bumps in VDOS/ω^2 plots near 100 cm^{-1} in all the samples. In ASi sample, there is a broad bump at around 95 cm^{-1} while in *a*-Si:H samples viz: ASiH, BSiH, CSiH and WSiH, it is around 107, 104, 105 and 105 cm^{-1}, respectively. The Raman scattering on bulk silicon[59] has also reported the peak at 114 cm^{-1}. We notice that the position of peak is almost independent of the sample and depends only on the type of sample whether pure or hydrogenated amorphous silicon. In *a*-Si:H samples, the height of peak is smaller as compared to that in pure amorphous silicon sample (ASi) which means that there is a decrease in the low frequency modes in amorphous silicon upon hydrogenation. Liu *et al.*[60] have also reported such a reduction in the low frequency modes in amorphous silicon upon hydrogenation.

The VDOS is further used to calculate the temperature (*T*) dependence of free energy, vibrational entropy and specific
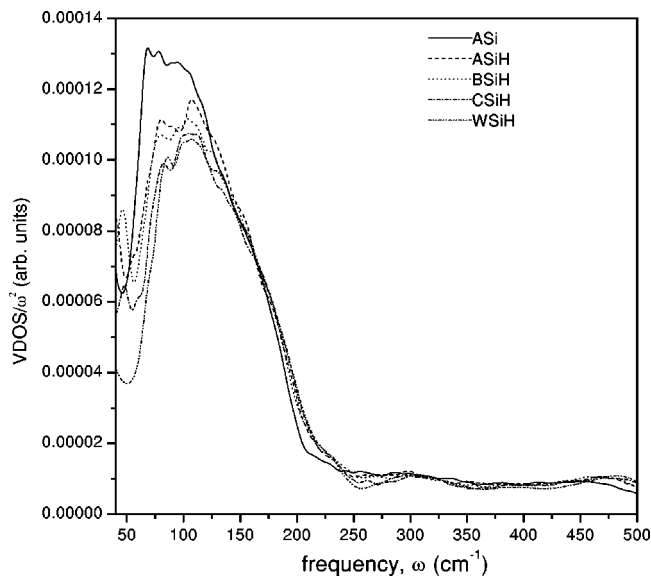
FIG. 8. VDOS/ω^2 versus ω for model samples of pure and hydrogenated amorphous silicon.

heat (C) with the help of Eqs. 2–4. The overall temperature dependence of specific heat for our samples is in good agreement with the Dulong and Petit's law at high temperatures. From Fig. 9, it is clear that while the free energy decreases, the entropy and specific heat increase with the increase in temperature in all the samples. In the a-Si:H samples, the free energy is more, whereas the entropy and specific heat are less than those of the pure amorphous silicon sample at all temperatures. However, the intercomparison of a-Si:H samples shows that in samples (ASiH, BSiH) prepared from the liquid quench, the free energy is smaller whereas the entropy and specific heat are larger as compared to that of samples (CSiH, WSiH) prepared by hydrogenation of pure amorphous silicon samples at all the temperatures. Since the entropy is the measure of disorder, the higher entropy of pure amorphous sample (ASi) indicates that it is more disordered compared to the hydrogenated samples. The comparison of entropy of hydrogenated samples shows that the samples generated from liquid quench are more disordered compared to other samples.

In Fig. 9(d), we have displayed C/T^3 versus T curves. The inset in Fig. 9(d) shows a clear bulge in these curves at low temperatures in all of our samples. The existence and position of this bulge in the specific-heat at low temperatures in our samples is in good agreement with the previous theoretical[61,62] and experimental results.[63] The height of the peak in the hydrogenated samples is lower as compared to that in the pure amorphous silicon sample. The comparison of heights of peak in the hydrogenated samples shows that it is lower in the samples (ASiH, BSiH) prepared by hydrogenation of pure amorphous silicon samples as compared to that in other samples prepared from the liquid quench. Although ASiH and BSiH samples have quite different coordination defects, they have almost identical peak heights in C/T^3 plots, while CSiH and WSiH samples have almost similar coordination defects but they have quite different peak heights in C/T^3 plots. This indicates no connection be-
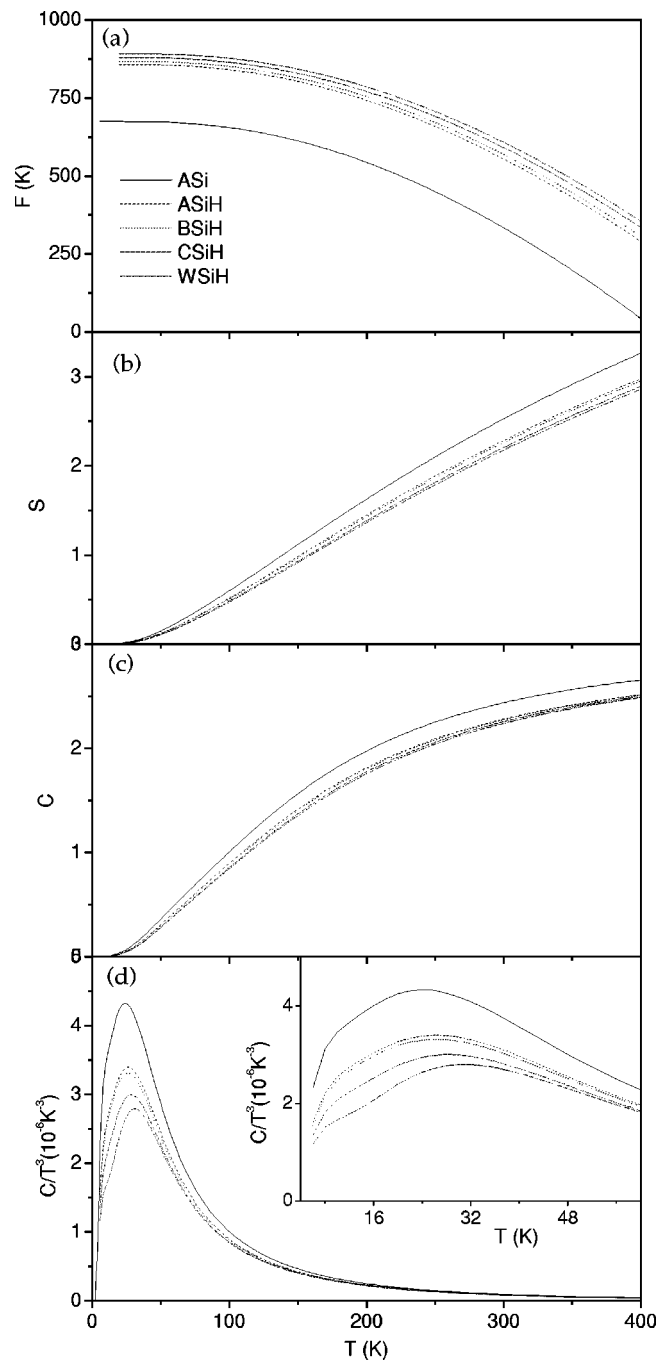

FIG. 9. The temperature (T) dependence of (a) free energy (F), (b) vibrational entropy (S) and (c) specific heat (C) calculated from the VDOS within the harmonic approximation. In (d), we have displayed C/T^3 versus T curves. The values along the y axis in all panels are per atom in units of k_B. The curve descriptions are the same in all the panels as given in (a).

tween coordination defects and the peak in specific heat at low temperatures.

C. Electronic properties

We have investigated the electronic properties of pure and hydrogenated amorphous silicon samples by calculating the
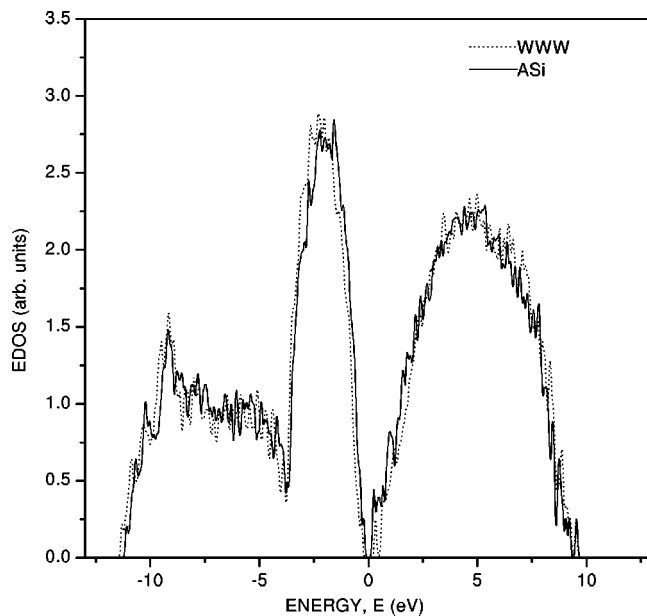
FIG. 10. Electronic density of states (EDOS) for ASi and WWW samples (Ref. 25) of pure amorphous silicon. $E=0$ eV corresponds to the Fermi level.

electronic density of states. The calculated results are given in Figs. 10 and 11. The energy, $E=0$ eV in all the panels of these figures corresponds to the Fermi level of the corresponding samples as shown in the panels. The electronic density of states shows a small energy gap at the Fermi level in all of our samples which is quite typical for such model structures as has also been found in various previous theoretical calculations.[6,64] The total electronic density of states (EDOS) of pure amorphous silicon samples (ASi and WWW) as given in Fig. 10 shows that there is a clear formation of a gap around the Fermi level in both the samples. The general shape of EDOS in both the samples is almost the same except that the band gap around the Fermi level is wider in WWW sample as compared to that in ASi sample. Thus there are more states in the gap region of ASi sample as compared to that in WWW sample. As is well known, these gap states are due to the presence of coordination defects. The ASi sample has about 9% coordination defects (both threefold and fivefold), while the WWW sample has only 0.1% fivefold defects. The shape of band tails near the gap region is exponential in both of these samples. Such an exponential behavior of band tail states in amorphous silicon has also been shown by Jianjun *et al.*.[65] and is a universal feature of amorphous semiconductors caused by the short range disorder in these materials.

The local electronic density of states of hydrogen atoms ($LDOS_H$) and Si atoms ($LDOS_{Si}$) and total electronic density of states (EDOS) for the a-Si:H samples are given in Fig. 11. For clarity we displayed them separately for each sample. In valance band region ($-10.0-0.0$ eV) $LDOS_H$ has a similar shape in all the samples but in the conduction band region ($0.0-10.0$ eV) has a different shape for the samples (ASiH, BSiH) generated from the liquid quench and for those (CSiH, WSiH) generated by hydrogenation of pure amorphous silicon samples. The general shape of $LDOS_{Si}$ at Si

sites and EDOS is almost the same in all of the four samples. The band tail states near band gap region in EDOS have almost the same exponential distribution as in the pure amorphous silicon sample. There is a decrease in the electronic band tail states in the gap region and increase in the energy gap around Fermi level in EDOS in the hydrogenated samples which is consistent with the earlier studies.[2] Balamurugan and Prasad[66] have also reported the increase of first excited electronic level gap in the small silicon clusters upon hydrogenation. There is a considerable decrease in the conduction band tail states near the band gap region and increase in the band gap in both the hydrogenated samples. Thus, hydrogenation has the tendency to remove the states from the gap region and increase the band gap.

IV. CONCLUSIONS

We have presented the DFTB based MD calculations for the sample dependence of structural, vibrational and electronic properties a-Si:H. The samples of a-Si:H are generated by quenching from the liquid state of silicon-hydrogen mixture and by hydrogenation of pure amorphous silicon samples. The overall structural properties of these model structures are in good agreement with the previous experimental and theoretical results. The a-Si:H samples generated from the liquid quench have more coordination defects as compared to the samples generated by hydrogenation of pure amorphous silicon. The Si-Si and Si-H pair correlations are found independent of preparation procedure and initial conditions, whereas the H-H pair correlations are sample dependent. It has been found that almost all the hydrogen atoms are bonded to silicon atoms, in Si-H monohydride fashion, existing either as isolated Si-H bond or as clusters of Si-H bonds. The distribution of hydrogen in all the samples is found nonuniform and depends upon the preparation procedure and the initial structure from which the hydrogenated sample is generated. The Si-Si bond length and Si-Si-Si bond angle distributions are nearly independent of sample preparation procedure, but Si-H bond length distributions are dependent.

The vibrational properties of these samples are investigated by calculating the VDOS and localization of vibrational modes. The VDOS of pure amorphous silicon sample is in good agreement with the experimental data. In hydrogenated samples, there exist extra peaks in the frequency range $600-2200$ cm^{-1} which are also in reasonable accord with the experimental results. In VDOS/ω^2 versus ω plot there occurs a peak at low frequencies in all of our samples. The position and height of this peak shows no connection to coordination defects. The height of this peak also indicates that the low frequency vibrational modes are less in the samples generated by hydrogenation of pure amorphous silicon samples as compared to the other samples generated from the liquid quench. While the high frequency modes related to Si-Si bond vibrations are found moderately localized both in pure and hydrogenated amorphous silicon, the vibrational modes related to Si-H vibrations are highly localized.

The VDOS is further used to calculate the temperature dependence of thermodynamic properties within the har-
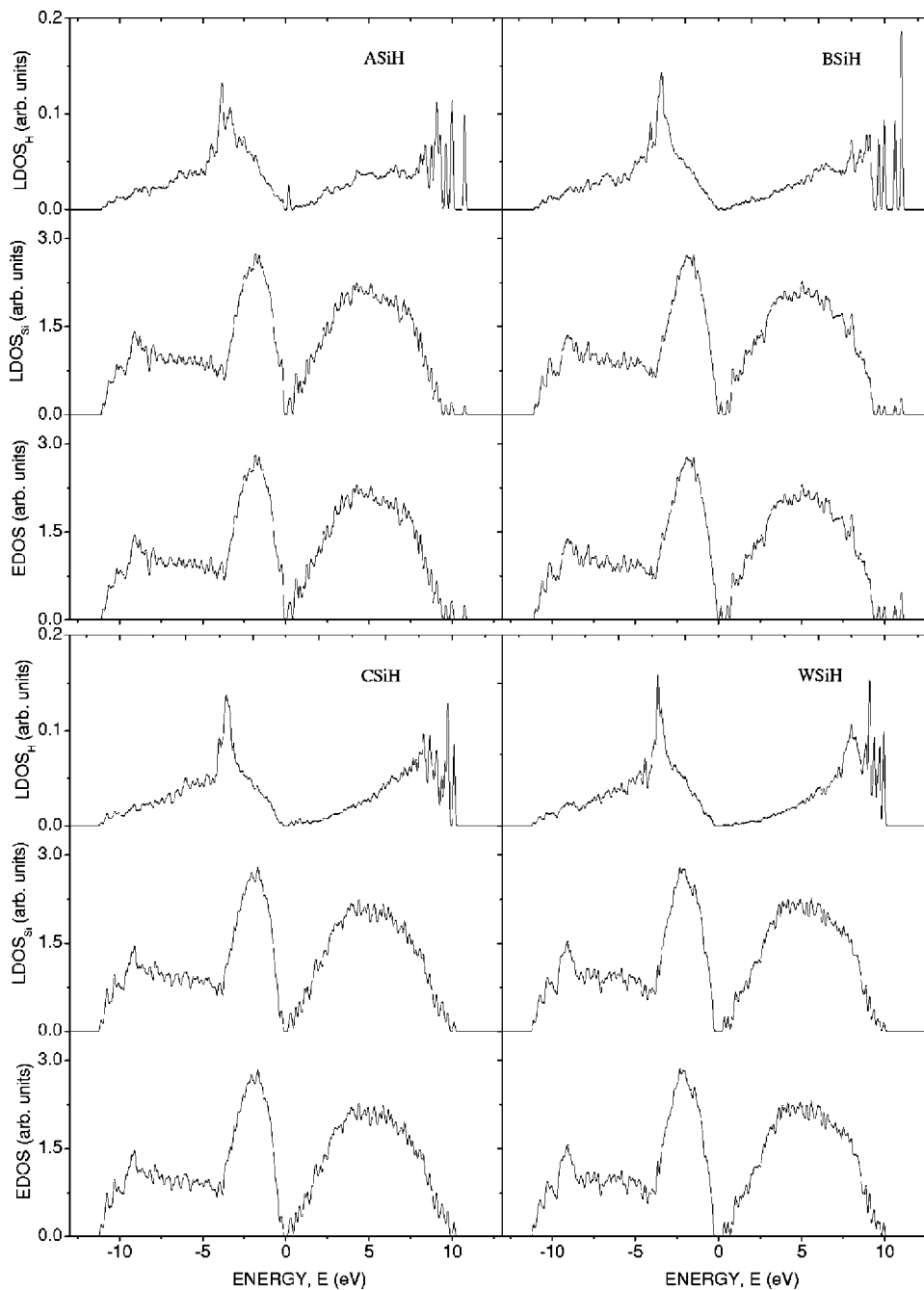
FIG. 11. The local electronic density of states of hydrogen atoms (LDOS$_H$) and silicon atoms (LDOSsi) and total electronic density of states (EDOS) for a-Si:H samples (ASiH, BSiH, CSiH and WSiH). For clarity these are displayed separately for each sample. E=0 eV corresponds to the Fermi level.

monic approximation. It has been found that the free energy decreases whereas the entropy and specific heat increase with increase in temperature in all samples. In a-Si:H samples, the free energy is larger while the entropy and specific heat are lower than that of pure amorphous silicon sample at all the temperatures. However, the intercomparison of a-Si:H samples shows that in samples prepared from the liquid quench, the free energy is smaller whereas the entropy and specific heat are larger as compared to that of samples prepared by hydrogenation of pure amorphous silicon samples at all temperatures. At low temperatures, there exists a bump in C/T^3 plots of all the samples. The height and position of this bump show no relation with the coordination defects. The electronic density of states shows a small energy gap at the Fermi level in all the samples. The hydrogenation of pure amorphous silicon reduces the electronic gap states and increases the energy gap. The total electronic density of states and local density of electronic states (LDOS) at Si atom sites are nearly sample independent, while the LDOS at the H atom sites is dependent on the sample preparation procedure.

[1] D. L. Staebler and C. R. Wronski, Appl. Phys. Lett. **31**, 292 (1977).

[2] See, for example, R. A. Street, *Hydrogenated Amorphous Silicon* (Cambridge University Press, Cambridge, 1991); *Physics of Hydrogenated Amorphous Silicon II*, edited by J. D. Joannopoulos and G. Lucovsky (Springer, New York, 1984); *Amorphous Silicon Semiconductors-Pure & Hydrogenated*, edited by D. Adler, Y. Hamakawa, A. Madan, and M. Thompson (Materials Research Society, 1987); *Hydrogenated Amorphous Silicon*, edited by H. Neber-Aeschbacher (Trans Tech, 1995).

[3] M. Peressi, M. Fornari, S. de Gironcoli, L. De Santis, and A. Baldereschi, Philos. Mag. B **80**, 515 (2000); R. O. Jones, B. W. Clare, and P. J. Jennings, Phys. Rev. B **64**, 125203 (2001); M. J. Powell, S. C. Deane, and R. B. Wehrspohn, *ibid.* **66**, 155212 (2002).

[4] C. W. Rella, M. van der Voort, A. V. Akimov, A. F. G. van der Meer, and J. I. Dijkhuis, Appl. Phys. Lett. **75**, 2945 (1999).

[5] M. van der Voort, C. W. Rella, L. F. G. van der Meer, A. V. Akimov, and J. I. Dijkhuis, Phys. Rev. Lett. **84**, 1236 (2000); M. van der Voort, A. V. Akimov, and J. I. Dijkhuis, Phys. Rev. B **62**, 8072 (2000); H. Oheda, *ibid.* **66**, 035201 (2002).

[6] M. Fornari, M. Peressi, S. de Gironcoli, and A. Baldereschi, Europhys. Lett. **47**, 481 (1999).

[7] V. Nádaždy, R. Durný, I. Thurzo, E. Pinčĺk, A. Nishida, J. Shimizu, M. Kumeda, and T. Shimizu, Phys. Rev. B **66**, 195211 (2002).

[8] R. Prasad and S. R. Shenoy, Phys. Lett. A **218**, 85 (1996).

[9] Y. Wu, J. T. Stephen, D. X. Han, J. M. Rutland, R. S. Crandall, and A. H. Mahan, Phys. Rev. Lett. **77**, 2049 (1996).

[10] S. Acco, D. L. Wlliamson, S. Roorda, W. G. J. H. M. van Sark, A. Polman, and W. F. van der Weg, J. Non-Cryst. Solids **227–230**, 128 (1998).

[11] D. L. Williamson, D. W. M. Marr, J. Yang, B. Yan, and S. Guha, Phys. Rev. B **67**, 075314 (2003).

[12] H. Touir, K. Zellama, and J. F. Morhange, Phys. Rev. B **59**, 10 076 (1999).

[13] P. A. Fedders, Phys. Rev. B **66**, 195308 (2002).

[14] T. Su, P. C. Taylor, G. Ganguly, and D. E. Carlson, Phys. Rev. Lett. **89**, 015502 (2002).

[15] R. Biswas, B. C. Pan, and Y. Y. Ye, Phys. Rev. Lett. **88**, 205502 (2002).

[16] S. C. Agarwal, Indian J. Pure Appl. Phys. **34**, 597 (1996).

[17] A. K. Sinha and S. C. Agarwal, J. Vac. Sci. Technol. B **18**, 1805 (2000).

[18] G. Pribil, Z. Hubicka, R. J. Soukup, and N. J. Ianno, J. Vac. Sci. Technol. A **19**, 1571 (2001); Surf. Coat. Technol. **160**, 114 (2002).

[19] *Plasma Deposition of Amorphous Silicon Based Materials*, edited by G. Bruno, P. Capezzuto, and A. Madan (Academic, New York, 1995).

[20] *Amorphous and Heterogeneous Silicon Thin Films-2000*, edited by R. W. Collins, H. M. Branz, S. Guha, H. Okamoto, and M. Stutzmann, MRS Symposia Proceedings No. 609 (Materials Research Society, Pittsburgh, 2000).

[21] F. H. Stillinger and T. A. Weber, Phys. Rev. B **31**, 5262 (1985).

[22] R. Biswas and D. R. Hamann, Phys. Rev. Lett. **55**, 2001 (1985).

[23] J. Tersoff, Phys. Rev. Lett. **56**, 632 (1986).

[24] G. B. Bachelet, D. R. Hamann, and M. Schlüter, Phys. Rev. B **26**, 4199 (1982).

[25] F. Wooten, K. Winer, and D. Weaire, Phys. Rev. Lett. **54**, 1392 (1985).

[26] G. T. Barkema and N. Mousseau, Phys. Rev. B **62**, 4985 (2000).

[27] R. Car and M. Parrinello, Phys. Rev. Lett. **60**, 204 (1985).

[28] R. Biswas, G. S. Grest, and C. M. Soukoulis, Phys. Rev. B **36**, 7437 (1987).

[29] W. D. Luedtke and U. Landman, Phys. Rev. B **40**, 1164 (1989).

[30] Q. Li and R. Biswas, Phys. Rev. B **50**, 18 090 (1994).

[31] R. L. C. Vink, G. T. Barkema, R. H. Bisseling, and M. A. Stijnman, Phys. Rev. B **64**, 245214 (2001); R. L. C. Vink (private communications).

[32] F. Buda, G. L. Chiarotti, R. Car, and M. Parrinello, Phys. Rev. B **44**, 5908 (1991); F. Buda, Ph.D. thesis, SISSA, Trieste, Italy, 1989.

[33] S. Zafar and E. A. Schiff, Phys. Rev. Lett. **66**, 1493 (1991).

[34] N. Mousseau and L. J. Lewis, Phys. Rev. B **43**, 9810 (1991).

[35] P. A. Fedders and D. A. Drabold, Phys. Rev. B **47**, 13 277 (1993).

[36] B. Tuttle and J. B. Adams, Phys. Rev. B **53**, 16 265 (1996).

[37] M. Elstner, D. Porezag, G. Jungnickel, J. Elsner, M. Haugk, Th. Frauenheim, S. Suhai, and G. Seifert, Phys. Rev. B **58**, 7260 (1998); Phys. Status Solidi B **217/1**, 41 (2000).

[38] P. Klein, H. M. Urbassek, and Th. Frauenheim Phys. Rev. B **60**, 5478 (1999).

[39] A. A. Maradudin, E. W. Montroll, G. H. Weiss, and I. P. Ipatova, *Theory of Lattice Dynamics in the Harmonic Approximation*, 2nd ed. (1971), p. 130.

[40] R. Biswas, A. M. Bouchard, W. A. Kamitakahara, G. S. Grest, and C. M. Soukoulis, Phys. Rev. Lett. **60**, 2280 (1988).

[41] H. J. Monkhorst and J. D. Pack, Phys. Rev. B **13**, 5188 (1976).

[42] K. Laaziri, S. Kycia, S. Roorda, M. Chicoine, J. L. Robertson, J. Wang, and S. C. Moss, Phys. Rev. B **60**, 13 520 (1999); Phys. Rev. Lett. **82**, 3460 (1999).

[43] R. Bellisent, A. Menelle, W. S. Howells, A. C. Wright, T. M. Brunier, R. N. Sinclair, and F. Jansen, Physica B **156&157**, 217 (1989).

[44] G. R. Gupte, R. Prasad, V. Kumar, and G. L. Chiarotti, Bull. Mater. Sci. **20**, 429 (1997).

[45] M. H. Brodsky, M. Cardona, and J. J. Cuomo, Phys. Rev. B **16**, 3556 (1977).

[46] G. Lucovsky, R. J. Nemanich, and J. C. Knights, Phys. Rev. B **19**, 2064 (1979).

[47] J. Baum, K. K. Gleason, A. Pines, A. N. Garroway, and J. A. Reimer, Phys. Rev. Lett. **56**, 1377 (1986); J. A. Reimer and R. W. Vaughan, Phys. Rev. B **24**, 3360 (1981); D. Han, J. Baugh, and G. Yue, *ibid.* **62**, 7169 (2000).

[48] A. H. M. Smets, W. M. M. Kessels, and M. C. M. van de Sanden, Appl. Phys. Lett. **82**, 1547 (2003).

[49] W. A. Kamitakahara, C. M. Soukoulis, H. R. Shanks, U. Buchenau, and G. S. Grest, Phys. Rev. B **36**, 6539 (1987).

[50] S. Nakhmanson and D. A. Drabold, Phys. Rev. B **58**, 15 325 (1998); S. Nakhmanson (private communications).

[51] S. Nakhmanson and D. A. Drabold, J. Non-Cryst. Solids **266–269**, 156 (2000).

[52] P. Biswas, Phys. Rev. B **65**, 125208 (2002).

[53] W. A. Kamitakahara, H. R. Shanks, and J. F. McClelland, Phys. Rev. Lett. **52**, 644 (1984).

[54] M. Ivanda, K. Furic, O. Gamulin, and D. Gracin, J. Non-Cryst. Solids **137&138**, 103 (1991).

[55] N. Mousseau and L. J. Lewis, Phys. Rev. B **41**, 3702 (1990).

[56] A. Langford, M. L. Fleet, B. P. Nelson, W. A. Lanford, and N. Maley, Phys. Rev. B **45**, 13 367 (1992); U. Kroll, J. Meier, A. Shah, S. Mikhailov, and J. Weber, J. Appl. Phys. **80**, 4971 (1996); R. Ossikovski and B. Drévillon, Phys. Rev. B **54**, 10 530 (1996).

[57] A. P. Sokolov, A. Kisluik, D. Quitman, A. Kudlik, and E. Rössler, J. Non-Cryst. Solids **172–174**, 138 (1994).

[58] V. K. Malinovsky, V. N. Novikov, P. P. Parshin, A. P. Sokolov, and M. G. Zemlyanov, Europhys. Lett. **11**, 43 (1990); S. Kojima and M. Kodama, Physica B **263–264**, 336 (1999); F. Finkemeier and W. von Niessen, Phys. Rev. B **63**, 235204 (2001).

[59] C. Laermans and M. Coeck, Physica B **263–264**, 280 (1999).

[60] X. Liu, B. E. White, Jr., R. O. Pohl, E. Iwanizcko, K. M. Jones, A. H. Mahan, B. N. Nelson, R. S. Crandall, and S. Veprek, Phys. Rev. Lett. **78**, 4418 (1997).

[61] J. L. Feldman, P. B. Allen, and S. R. Bickham, Phys. Rev. B **59**, 3551 (1999).

[62] S. M. Nakhmanson and D. A. Drabold, Phys. Rev. B **61**, 5376 (2000).

[63] M. Mertig, G. Pompe, and E. Hegenbarth, Solid State Commun. **49**, 369 (1984).

[64] R. Biswas, C. Z. Wang, C. T. Chan, K. M. Ho, and C. M. Soukoulis, Phys. Rev. Lett. **63**, 1491 (1989); P. Klein, H. M. Urbassek, and T. Frauenheim, Phys. Rev. **60**, 5478 (1999); V. I. Ivashchenko, P. E. A. Turchi, V. I. Shevchenko, L. A. Ivashchenko, and G. V. Rusakov, J. Phys.: Condens. Matter **15**, 4119 (2003).

[65] J. Dong and D. A. Drabold, Phys. Rev. Lett. **80**, 1928 (1998).

[66] D. Balamurugan and R. Prasad, Phys. Rev. B **64**, 205406 (2001).